IEEE Access
Multidisciplinary | Rapid Review | Open Access Journal

Received February 1, 2018, accepted March 21, 2018, date of publication April 25, 2018, date of current version June 5, 2018.

Digital Object Identifier 10.1109/ACCESS.2018.2829984

A Time Reversal Based Pipeline Leakage Localization Method With the Adjustable Resolution

GUANGMIN ZHANG[1], JUNXIAO ZHU[2], YUE SONG[1], CHAO PENG[1], AND GANGBING SONG[2,3]

[1]School of Electrical Engineering and Intelligentization, Dongguan University of Technology, Dongguan, 523808, China.
[2]Department of Mechanical Engineering, University of Houston, Houston, TX 77204, USA.
[3]School of Environment and Civil Engineering, Dongguan University of Technology, Dongguan, 523808, China

Corresponding author: Gangbing Song (gsong@central.uh.edu)

This work was supported in part by the Major State Basic Research Development Program of China (973 Program) under Grant 2015CB057704, in part by the General Project of the National Natural Science Foundation of China under Grant 51478080, in part by the Ph.D. Start-up Fund of the Natural Science Foundation of Guangdong Province, China, under Grant 2014A030310271, in part by the Foundation for Distinguished Young Talents in Higher Education of Guangdong, China, under Grant 2014KQNCX216, and in part by the Dongguan Municipal Science and Technology Bureau under Grant 2016508140.

ABSTRACT Due to the diffraction limit, the systems to localize signal sources used to suffer from the low resolution issue, which also occurs in the pipeline leakage localization. For a pressurized pipeline that carries gas, a leakage will generate a negative pressure wave (NPW) that propagates along the pipeline. The NPW can be detected by piezoceramic transducers that are bonded on the surface of the pipeline. Via processing NPW signals, the locations of the leakages can be obtained. However, since the wavelengths of the NPW signals are several meters, the resolution is meter sized. In this paper, a novel pipeline leakage localization method which can adjust the resolution is developed to improve the localization resolution. The proposed method includes a formula to adjust the localization resolution based on the time reversal technique. Via adjusting the parameter of the formula, various localization resolutions can be obtained. We investigated the performance of the proposed method in an experiment with a 55.8 m PVC pipeline equipped with two manually controllable leakage points. With the help of the piezoceramic transducers, the experimental results show that the proposed method can deliver the resolutions which represent a significant improvement, as compared with that of the conventional time reversal localization method. Furthermore, the proposed method can be used for other passive detection.

INDEX TERMS Negative pressure wave, resolution, localization, piezoceramic transducer, time reversal technique, pipeline.

I. INTRODUCTION

Recently, various techniques have been developed for structure health monitoring (SHM) [1]–[3] For example, the structural damage detection based on the electromechanical impedance [4]–[7] and vibration modal shape [8]–[10] were investigated. Among the SHM methods, the ones based on the waves can reveal a variety of characteristics of the defects, such as position and size. For example, Huang and Bednorz introduced S-parameter measurement to the ultrasound inspection of the aluminum plate [11]. In addition, the block-sparse imaging method [12], the phased array imaging method [13] and the delay-and-Boolean-ADD imaging algorithm [14] are used to process ultrasonic signals to localize the defect. Since the ultrasonic signal and the electromagnetic signal have the spatial reciprocity, the time-reversal imaging algorithm can give the damages' location, when it is used to process the ultrasonic or electromagnetic signals from damages [15], [20]. Gao *et al.* [16]. analyzed the guide waves propagation characteristics by using the local probability-based diagnostic imaging method to inspect the multi-damage in an aluminum plate. Hosseinabadi *et al.* [17] used the damage-sensitive features of the guided ultrasonic wave signals to establish a multiple-input multiple-output fixed grid wavelet network, and trained the wavelet network to identify the structural damage. Lin*et al.* [18] developed an excitation waveform design strategy based on pulse

compression to meet the demands of high-resolution Lamb wave inspection in composite materials. An *et al.* [19] developed an ultrasonic wavefield imaging method to detect hidden damages. A wavelet packet-based ultrasonic energy analysis was developed to distinguish the type of cracks [21]. However, most of investigations about the SHM methods based on the wave signal processing focus on active sensing which have to use a signal transceiver to obtain the signals from the defects. Little research on passive sensing approach has been conducted, especially the passive localization of the pipeline leakage [22]–[31]. The pipeline leakage passive localization methods based on the signals generated by the occurrence of leakage generally fall into two categories. One is the localization method based on negative pressure wave (NPW) [24]–[27], [30]. Jia *et al.* [24] used the hoop strain caused by the NPW to develop an approach to localize leaks. Zhao *et al.* [25] developed a method on the basis of wavelet transform to derive the position of the leak point. Hou *et al.* [26] developed a modified leak location formula based on the Compound Simpson formula and Dichotomy Searching. Hu *et al.* [27] developed a leak location approach which uses harmonic wavelet to process the NPW signal with high noise. The other is the acoustic based localization method [28], [29], [31]. Liu *et al.* [28] modified the propagation theory based on the dominant-energy frequency method to process the leak's acoustic signal. Giunta *et al.* [29] combined vibroacoustic sensing technique with wavelet analysis to reach leakage detection and localization in the laboratory.

However, for all wave signals including NPW, due to the lack of spatial high frequency components, the resolution of the localization methods based on wave signals is limited to the Rayleigh criterion of about 0.5λ (λ is the central wavelength of the spectrum), namely, the maximum -3 dB width is equal to half of the wavelength [32]–[35]. Furthermore, the wavelength of the NPW is several meters. Therefore, the NPW localization resolution which is highly related to the question of the size of the leak areas, used to be meter sized [32].

A common way to improve localization resolution is to use the so-called Locally Resonant MetaMaterials (LRMM) which can increase the spatial high frequency components [33]–[40]. Some LRMMs are made of a multilayered dielectric. Liao *et al.* [33] used a multilayered dielectric slab to obtain a resolution of 0.4λ. Gong *et al.* [34] enhanced the resolution to 0.1λ by using a grating plate. Some LRMMs are made of numbers of metallic rods or strips. For example, Rupin *et al.* [35] designed a LRMM composed of 100 long aluminum rods (61 cm long, 6.35 mm in diameter) and improved the resolution to $\lambda/6.2$. Li *et al.* [36] demonstrated that the LRMM made of a lattice of 3×10 metallic cylinders supports the enhancement of the information capacity of a localization system, a resolution of $\lambda/20$ is obtained. Gao *et al.* [37] developed the planar resonant lenses consisting of six substrates with periodically distributed strip resonators of various lengths and obtained a resolution of $\lambda/20$.

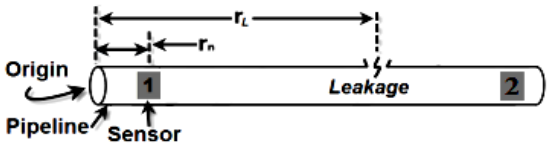

FIGURE 1. A pipeline with a leakage and the surface-bonded PZT sensors.

Another parts of LRMMs are composed of split-ring resonators. Wang *et al.* [38] claimed that a LRMM consist of split-ring resonators whose size is $0.1\lambda \times 0.1\lambda$, can enhance the resolution to 0.1λ. Ates *et al.* [39] designed split ring resonators to boost the transmission efficiency of the evanescent, and got a resolution of $\lambda/29$. Grbic *et al.* [40] developed a LRMM which consists of 5×19 grids of printed copper strips (microstrip transmission lines) loaded with series chip capacitors C and shunt (to the ground) chip inductors L, and obtained a resolution of 0.21λ. Although the method based on LRMM can improve the resolution, they have to use the additional devices (LRMMs) which will increase the hardware cost of the localization system. Furthermore, once the configurations of LRMMs are fixed, the resolution based on the LRMMs is nonadjustable. Therefore, the method is less practicable for actual localization application, such as pipeline leakage localization.

In this paper, a new leakage localization method with adjustable resolutions is developed for a pipeline. The proposed method includes a time reversal localization resolution adjustment formula. By adjusting the parameter of the formula and designing the corresponding localization background function, the proposed method can provide various localization resolutions without using any additional devices. For studying the performance of the proposed method in passive localization applications, a pipeline leakage localization experiment was executed. Two surface-bonded Lead Zirconate Titanate (PZT) transducers are used to detect the propagation of the NPW. PZT is a type of piezoceramic material with strong piezoelectric effect and is adopted in this research. The experimental results show that the two leakage locations along a 55.8m PVC pipeline can be identified accurately by using the proposed method. Furthermore, the conventional localization method can only offer a resolution of about 5.5m. Meanwhile, by using the proposed method, the resolution can be adjustable, and the minimum resolution can even be 3cm in this experiment.

II. THEORY OF THE PROPOSED METHOD

Shown in Figure 1 is a pipeline with a leakage. Two PZT sensors are bonded on the pipeline near both ends. For a pressurized pipeline that carries gas, a leakage will generate a NPW that will propagate along the pipeline. The NPW will be detected by piezoceramic transducers that are bonded on the surface of the pipeline.

We assume that the n^{th} sensor is located at $\mathbf{r_n}$. We further assume that the leakage happens at $\mathbf{r_L}$, and generates a NPW signal $e(\mathbf{r_L}, t)$. In this paper, plain symbols denote

scalar quantities, whereas vectors and matrices are denoted by bold symbols. Assume the leakage generates an NPW signal at time $t = T_{\mathbf{L}}$ All sensors are synchronous.

Assume the channel impulse response from $\mathbf{r_L}$ to $\mathbf{r_n}$ is,

$$h_{\mathbf{m}}(\mathbf{r_n}, \mathbf{r_L}, t) = a_{\mathbf{n,L,m}}\delta(t - t_{\mathbf{n,L,m}}) \tag{1}$$

where $a_{\mathbf{n,L,m}}$ is the attenuation coefficient between $\mathbf{r_L}$ and $\mathbf{r_n}$, $\delta\left(t - t_{\mathbf{n,L,m}}\right)$ is the ideal impulse signal, $t_{\mathbf{n,L,m}}$ is the propagation delay time of the NPW from $\mathbf{r_L}$ to $\mathbf{r_n}$, The subscript "m" corresponds to the forward propagation fields, measured via the experiment.

The leakage signal recorded by the n^{th} sensor can be modeled as,

$$x(\mathbf{r_n}, \mathbf{r_L}, t) = e(\mathbf{r_L}, t) * h_{\mathbf{m}}(\mathbf{r_n}, \mathbf{r_L}, t) * \delta(t - T_{\mathbf{L}}) \tag{2}$$

where "$*$" represents the convolution operation.

The cross-correlation function $y(t)$ between $x(\mathbf{r_1}, \mathbf{r_L}, t)$ and $x(\mathbf{r_2}, \mathbf{r_L}, t)$ is computed as,

$$\begin{aligned} y(t) &= x(\mathbf{r_1}, \mathbf{r_L}, t) * x(\mathbf{r_2}, \mathbf{r_L}, -t) \\ &= e(\mathbf{r_L}, t) * e(\mathbf{r_L}, -t) \\ &\quad * a_{\mathbf{1,L,m}}a_{\mathbf{2,L,m}}\delta(t - t_{\mathbf{1,L,m}} + t_{\mathbf{2,L,m}}) \end{aligned} \tag{3}$$

Then, the self-correlation function $y'(t)$ of $x(\mathbf{r_1}, \mathbf{r_L}, t)$ is computed as,

$$\begin{aligned} y'(t) &= x(\mathbf{r_1}, \mathbf{r_L}, t) * x(\mathbf{r_1}, \mathbf{r_L}, -t) \\ &= e(\mathbf{r_L}, t) * e(\mathbf{r_L}, -t) * a_{\mathbf{1,L,m}}a_{\mathbf{1,L,m}}\delta(t) \end{aligned} \tag{4}$$

Assume function $h'_{\mathbf{1,L,2}}(t)$ satisfies the following equation,

$$y(t) = y'(t) * h'_{\mathbf{1,L,2}}(t) \tag{5}$$

With using Fourier transform, $h'_{\mathbf{1,L,2}}(t)$ can be computed as,

$$h'_{\mathbf{1,L,2}}(t) = \frac{a_{\mathbf{2,L,m}}}{a_{\mathbf{1,L,m}}}\delta(t - t_{\mathbf{1,L,m}} + t_{\mathbf{2,L,m}}) \tag{6}$$

The amplitude normalization and the $\boldsymbol{p}$-1 time self-convolution are applied to $h'_{\mathbf{1,L,2}}(t)$ to obtain $s_{\mathbf{12}}(t)$, named as time reversal localization resolution adjustment function.

$$s_{\mathbf{12}}(t) = \delta(t - p \times t_{\mathbf{1,L,m}} + p \times t_{\mathbf{2,L,m}}) \tag{7}$$

Using $s_{\mathbf{12}}(t)$, we can re-write $x(\mathbf{r_1}, \mathbf{r_L}, t)$ and $x(\mathbf{r_2}, \mathbf{r_L}, t)$ as,

$$\begin{aligned} x'(\mathbf{r_1}, \mathbf{r_L}, t) &= x(\mathbf{r_1}, \mathbf{r_L}, t) * s_{\mathbf{12}}(-t) \\ &= e(\mathbf{r_L}, t) * a_{1,\mathbf{L,m}}\delta(t - T_{\mathbf{L}} + (p-1) \\ &\qquad \times t_{\mathbf{1,L,m}} - p \times t_{\mathbf{2,L,m}}) \end{aligned} \tag{8}$$

$$\begin{aligned} x'(\mathbf{r_2}, \mathbf{r_L}, t) &= x(\mathbf{r_2}, \mathbf{r_L}, t) * s_{\mathbf{12}}(t) \\ &= e(\mathbf{r_L}, t) * a_{\mathbf{2,L,m}}\delta(t - T_{\mathbf{L}} - p \\ &\qquad \times t_{\mathbf{1,L,m}} + (p-1) \times t_{\mathbf{2,L,m}}) \end{aligned} \tag{9}$$

Designate the localization background functions for $x'(\mathbf{r_1}, \mathbf{r_L}, t)$ and $x'(\mathbf{r_2}, \mathbf{r_L}, t)$. At a generic observation point $\mathbf{r_k}$ of the monitoring area, the localization background functions of $x'(\mathbf{r_1}, \mathbf{r_L}, t)$ is written as,

$$h_{\mathbf{c}}(\mathbf{r_1}, \mathbf{r_k}, t) = \delta(t + (p-1) \times t_{\mathbf{1,k,c}} - p \times t_{\mathbf{2,k,c}}) \tag{10}$$

and the localization background functions of $x'(\mathbf{r_2}, \mathbf{r_L}, t)$ is written as

$$h_{\mathbf{c}}(\mathbf{r_2}, \mathbf{r_k}, t) = \delta(t + (p-1) \times t_{\mathbf{2,k,c}} - p \times t_{\mathbf{1,k,c}}) \tag{11}$$

where $t_{\mathbf{1,k,c}}$ is the propagation delay time of NPW from $\mathbf{r_k}$ to $\mathbf{r_1}$, $t_{\mathbf{2,k,c}}$ is the propagation delay time of NPW from $\mathbf{r_k}$ to $\mathbf{r_2}$, The subscript"c" represents that this corresponds to the back-propagation fields, obtained by calculation.

Then $x'(\mathbf{r_1}, \mathbf{r_L}, t)$ and $x'(\mathbf{r_2}, \mathbf{r_L}, t)$ are time reversed, and virtually back-propagated from the transducer as if it was able to act as a source (the proposed method employs convolution computation with the corresponding localization background functions to realize the back-propagation of the time reversed signals). Then, the signal obtained at the generic observation point $\mathbf{r_k}$ can be represented as,

$$q(\mathbf{r_k}, t) = \sum_{n=1}^{2} x'(\mathbf{r_n}, \mathbf{r_L}, -t) * h_{\mathbf{c}}(\mathbf{r_n}, \mathbf{r_k}, t) \tag{12}$$

When the computational data matches the measured one, namely $t_{\mathbf{n,k,c}} = t_{\mathbf{n,k,m}}$, (12) is a consequence of the reversibility property of the wave equation which implies that a maximum of energy is found on the point where the source was. Therefore, the leakage can be localized via plotting the maximum energy distribution curve of the monitoring area,

$$I_o(\mathbf{r_k}) = Max(\sum_{n=1}^{2} x'(\mathbf{r_n}, \mathbf{r_L}, -t) * h_{\mathbf{c}}(\mathbf{r_n}, \mathbf{r_k}, t)) \tag{13}$$

III. EXPERIMENTAL RESULTS

The full model pipeline was composed by a series of PVC pipe sections with a total length of 55.8m, as shown in Figure 2. The pipeline had six 9.1m straight sections which were connected by ten 90°-elbow connectors and five 0.2m sections. Two PZT sensors (15mm × 10mm × 0.4mm) were bonded on the outer surfaces of the pipeline. They are 1.32m and 54.46m away from the starting end. Two manually controllable valves are respectively located at 24.84m and 34.21m from the starting end. Opening any one of the valves simulates a leakage. Air was pumped into the pipeline by a compressor and a pressure regulator was used to regulate the pipeline pressure. For the safety reason, an automatic pressure release was employed. An event of leakage can be created by opening a valve on the pipeline. Then, the NPW signals generated by the leakages can be detected by the PZT sensors. An NI PXI-5105 Digitizer was used as a data acquisition system. The digitizer was triggered by the voltage signal of the sensor 1 with a −0.02V trigger level. The sampling rate of the data acquisition system is 100KS/s. The NPW velocity is considered as 300m/s [24], [30]. A signal conditioning circuit proposed in [30] was introduced to process the output voltages of the PZT sensors. Since the signal conditioning circuit works as a band pass filter [30], the output voltage of PZT sensor can keep being zero if there is no NPW reaching the location of the PZT sensor.

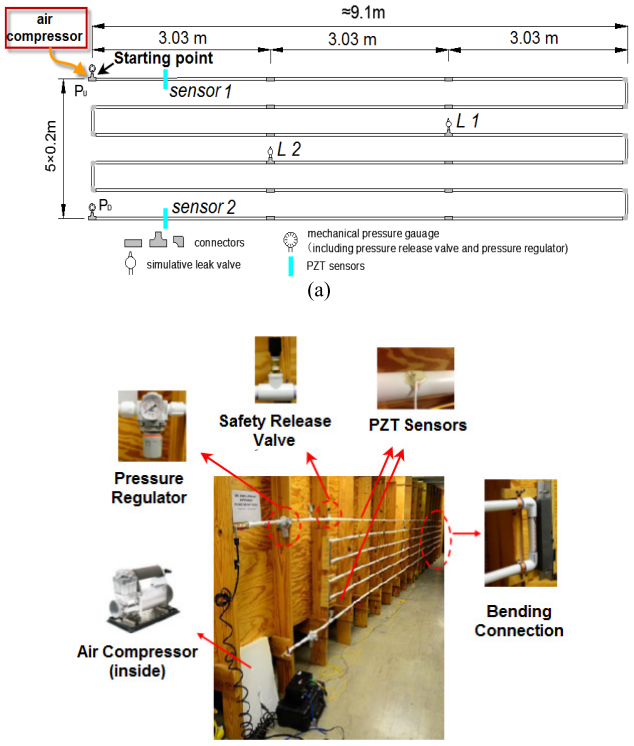

FIGURE 2. Schematic diagram and photo of the pipeline experiment. (a) The schematic diagram of the pipeline with PZT sensors. (b) A photo of the pipeline.

The internal pressure at the leakage point drops significantly as a result of pipeline content escaping through the leakage point. The pipeline content moves from both upstream and downstream simultaneously towards the leakage point. This flow of content generates a negative pressure wave propagating through the pipeline contents from the leakage point towards both ends of the pipeline. This decrease in pressure inside the pipeline is accompanied by the contraction of pipe's circumference resulting in strain variation on the pipe wall.

Due to the strain variation, the piezoelectric material directly mounted on the pipeline wall generates a corresponding electric signal. As shown in Figure 3, before the leakage happened, the signal captured by the sensor is 0 V because the internal pressure keeps constant under the normal operating conditions. Then, the downward, pulse-like waveform is generated due to the arrival of the NPW to sensors. The initial downward edge of the pulse indicates the decrease of internal pressure associated with the NPW. The upward edge of the pulse indicates the internal pressure settling at a different baseline pressure. The negative peak of the waveform indicates the NPW passes through the PZT sensor location. Finally, when the internal pressure settles down, low frequency signals dominate the PZT sensor, and a circuitry which works as a band pass causes the output amplitude to returns to 0 V.

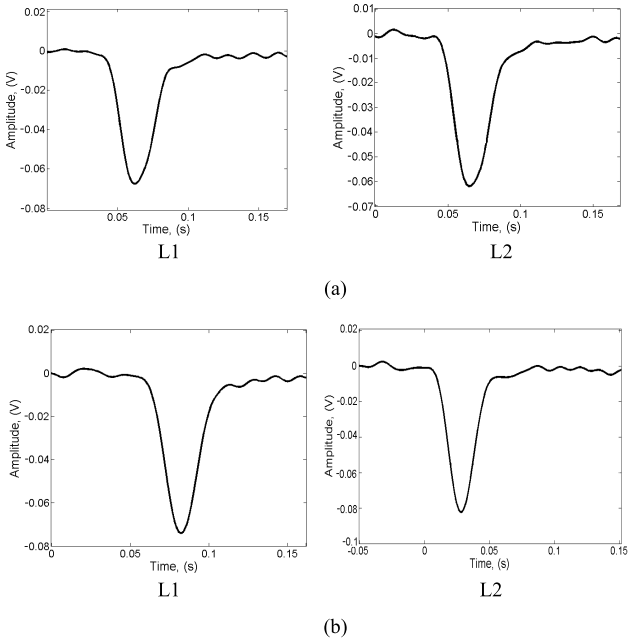

FIGURE 3. The signals captured by the two PZT sensors. (a) Sensor 1. (b) Sensor 2.

The conventional time reversal (TR) localization method [32] and the proposed method identify the leakage locations by using the maximum signal amplitude. Therefore, the amplitude of the measured data is inverted, before it is processed by using the both methods. The results based on the both methods are shown in Figure 4 The parameter $\boldsymbol{p}$ in (7) is set at various values in order to investigate the influence of the time reversal localization resolution adjustment function. From Figure 4, it can be seen that the three curves focus at the leakage positions. For such focusing patterns, their -3 dB width is a main feature, since this feature defines the resolution which is highly related to the question of the size of the leak areas. In other word, the -3 dB width sets a boundary limit between points having different signatures by using a special value chosen here at 0.7 (-3 dB). Apparently, both methods can correctly reveal the positions of the leakages by identifying the peaks of the three curves. However, the -3 dB widths of the curves based on the conventional time reversal localization method are much wider than those based on the proposed method when the parameter $\boldsymbol{p}$ in (7) is larger than one. Furthermore, the -3 dB width based on the proposed method gets narrow with the increase of the parameter $\boldsymbol{p}$.

Table 1 describes the energy peak's locations and -3 dB widths based on the two localization methods in detail. The peaks of the curves based on the conventional time reversal localization method are localized at 24.84m and 33.34m, with the -3dB widths are 5.55m and 5.65m respectively. The same curve peak locations can be observed in the results of the proposed method with various the parameter $\boldsymbol{p}$. That means that the both methods can identify the positions of the leaks. On the other hand, the minimum -3dB width of the conventional time reversal localization method is 5.55m. Meanwhile,

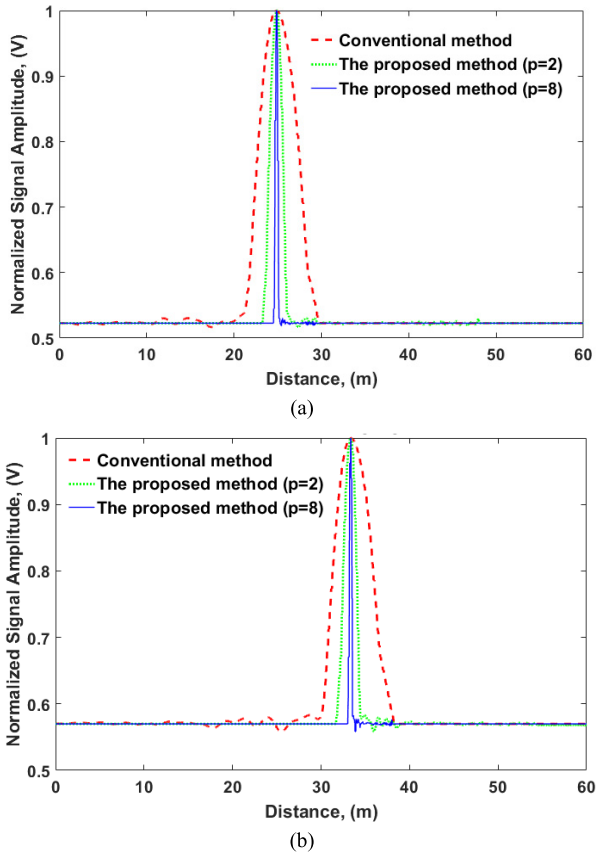

FIGURE 4. The maximum energy distribution curve based on the two methods. (a) L1. (b) L2.

TABLE 1. The energy peak's locations and −3dB widths based on the two localization methods.

	L 1		L 2	
	−3 dB width	Energy peak's location	−3 dB width	Energy peak's location
TR	22.28m~27.83m	24.84m	30.83m~36.49m	33.34m
p=8	24.64m~25.00m	24.84m	33.20m~33.50m	33.34m
p=20	24.76m~24.90m	24.84m	33.26m~33.40m	33.34m
p=50	24.81m~24.86m	24.84m	33.31m~33.36m	33.34m
p=80	24.82m~24.85m	24.84m	33.32m~ 33.35m	33.34m

the proposed method can provide a −3dB width of 0.03m which is 0.541% of that of the conventional TR localization method, when the parameter p=80, as shown in Figure 5.

IV. DISCUSSION

To explain the reason why the resolution is improved, the output values of the two methods at any generic observation point are investigated. Consider a generic observation point $\mathbf{r_z}$ which is close to the leakage, the NPW propagation delay time from $\mathbf{r_z}$ to $\mathbf{r_n}$ is $t_{\mathbf{n,z,c}}$. Consider $t_{\mathbf{n,z,c}} = t_{\mathbf{n,L,c}} + \Delta t_{\mathbf{n,z,L}}$.

For the conventional time reversal localization method, the equation described in [32] is used for analysis,

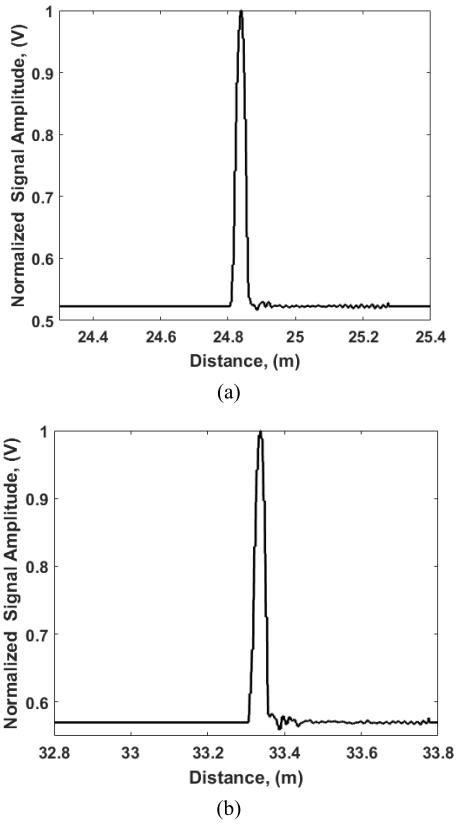

FIGURE 5. The maximum energy distribution curve based on the proposed method with p=80. (a) L1. (b) L2.

namely,

$$I_c(\mathbf{r_z}) = Max(\sum_{n=1}^{2} x(\mathbf{r_n}, \mathbf{r_L}, -t) * h'_{\mathbf{c}}(\mathbf{r_n}, \mathbf{r_z}, t)) \quad (14)$$

where $h'_{\mathbf{c}}(\mathbf{r_n}, \mathbf{r_z}, t)$ is the channel impulse response from $\mathbf{r_z}$ to $\mathbf{r_n}$, and $h'_{\mathbf{c}}(\mathbf{r_n}, \mathbf{r_z}, t) = \delta(t - t_{\mathbf{n,z,c}})$.

At the generic observation point $\mathbf{r_z}$, the output value of the conventional TR localization method can be written as

$$\begin{aligned} I_c(\mathbf{r_z}) = Max \big(&a_{\mathbf{1,L,m}} e(\mathbf{r_L}, -t) * \delta(t + T_{\mathbf{L}} + \Delta t_{1,\mathbf{z,L}}) \\ &+ a_{\mathbf{2,L,m}} e(\mathbf{r_L}, -t) * \delta(t + T_{\mathbf{L}} + \Delta t_{2,\mathbf{z,L}})\big) \end{aligned} \quad (15)$$

At the generic observation point $\mathbf{r_z}$, the output value of the proposed method can be written as

$$\begin{aligned} I_o(\mathbf{r_z}) = Max \big(&a_{\mathbf{1,L,m}} e(\mathbf{r_L}, -t) \\ &* \delta(t + T_{\mathbf{L}} + (p-1)\Delta t_{1,\mathbf{z,L}} - p\Delta t_{2,\mathbf{z,L}}) \\ &+ a_{\mathbf{2,L,m}} e(\mathbf{r_L}, -t) \\ &* \delta(t + T_{\mathbf{L}} + (p-1)\Delta t_{2,\mathbf{z,L}} - p\Delta t_{1,\mathbf{z,L}})\big) \end{aligned} \quad (16)$$

Since two transducers are set at the two ends of the pipeline, when the generic observation point $\mathbf{r_z}$ is closer to one end, the point will be far away from the other by the same distance. That means $\Delta t_{1,\mathbf{z,L}} = -\Delta t_{2,\mathbf{z,L}}$. Therefore, (15) and (16) can be re-written as,

$$\begin{aligned} I_c(\mathbf{r_z}) = Max \big(&a_{\mathbf{1,L,m}} e(\mathbf{r_L}, -t - T_{\mathbf{L}} - \Delta t_{1,\mathbf{z,L}}) \\ &+ a_{\mathbf{2,L,m}} e(\mathbf{r_L}, -t - T_{\mathbf{L}} + \Delta t_{1,\mathbf{z,L}})\big) \end{aligned} \quad (17)$$

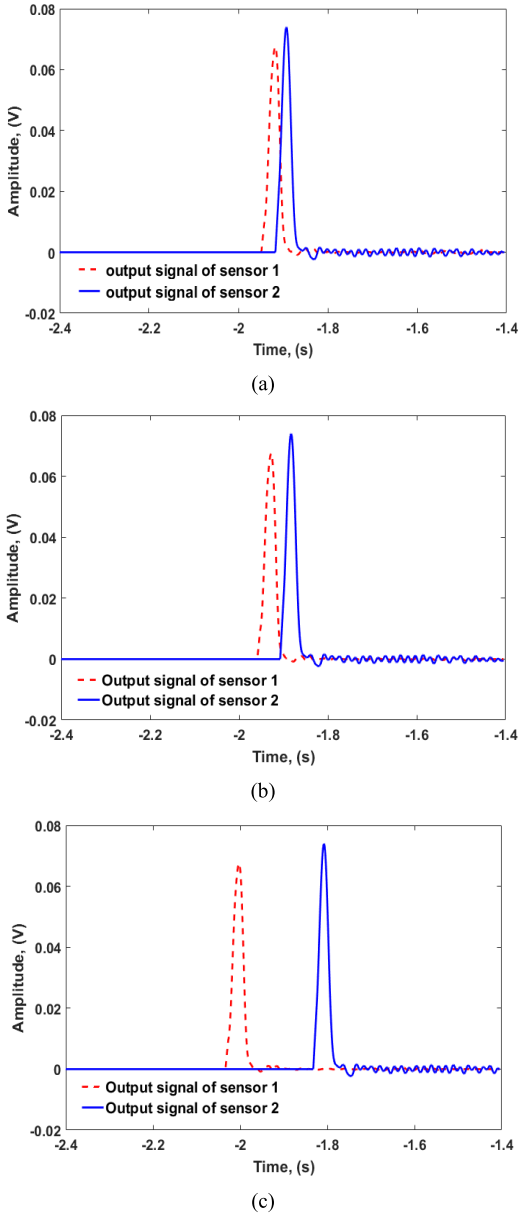

FIGURE 6. The two sensors' output signals of the proposed method with various parameter p at 25.6m for leakage L1. (a) p=3. (b) p=5. (c) p=20.

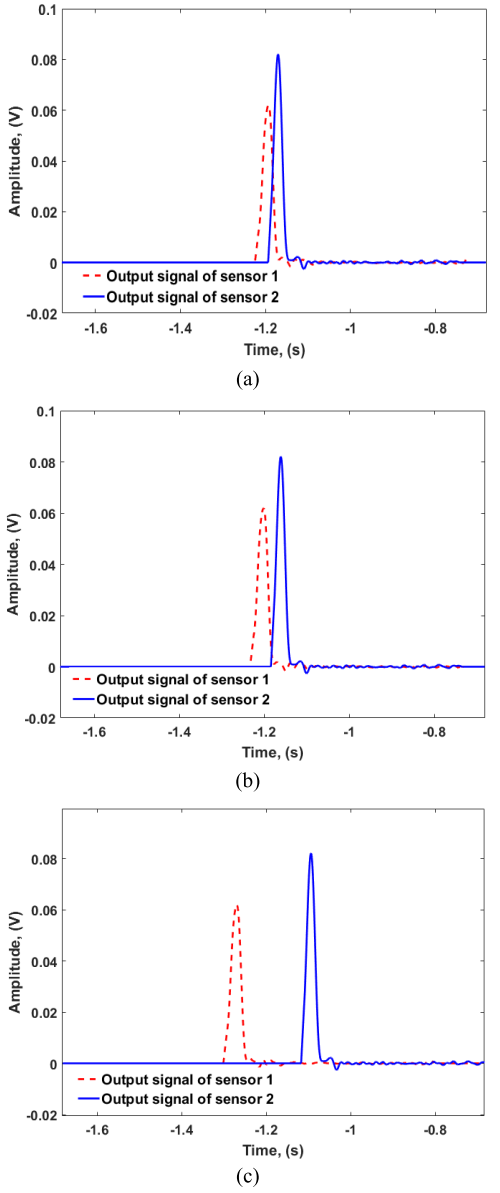

FIGURE 7. The two sensors' output signals of the proposed method with various parameter p at 34m for leakage L2. (a) p=3. (b) p=5. (c) p=20.

$$I_o(\mathbf{r_z}) = Max\left(a_{\mathbf{1,L,m}}e(\mathbf{r_L}, -t - T_\mathbf{L} - (2p-1)\Delta t_{1,\mathbf{z,L}}) + a_{\mathbf{2,L,m}}e(\mathbf{r_L}, -t - T_\mathbf{L} + (2p-1)\Delta t_{1,\mathbf{z,L}})\right) \quad (18)$$

The two signal components contained in (18), namely $a_{\mathbf{1,L,m}}e(\mathbf{r_L}, -t-T_\mathbf{L}-(2p-1)\Delta t_{1,\mathbf{z,L}})$ and $a_{\mathbf{2,L,m}}e(\mathbf{r_L}, -t-T_\mathbf{L}+(2p-1)\Delta t_{1,\mathbf{z,L}})$ are from sensor 1 and sensor 2, respectively. The time interval between the two components is $(4p-2)\Delta t_{1,\mathbf{z,L}}$. Since $(4p-2)\Delta t_{1,\mathbf{z,L}}$ increases with the increase of the parameter $\boldsymbol{p}$, the components can keep away from each other in time domain by increasing the parameter $\boldsymbol{p}$. To demonstrate this, the output signals of the proposed method with various parameter $\boldsymbol{p}$, at 25.6m and 34m are shown in Figures 6 and 7. At the observation points, the output signals of the two sensors become further away from each other with the increase of the parameter $\boldsymbol{p}$. As a result, the superposition energy of the two signals decrease with the increase of $\boldsymbol{p}$ The peak value of the output signal will decrease at the observation point. The area covered by the -3dB width becomes less, and the resolution is improved.

On the other hand, in (17), The time interval between the signal component $a_{\mathbf{1,L,m}}e(\mathbf{r_L}, -t-T_\mathbf{L}-\Delta t_{1,\mathbf{z,L}})$ and the signal component $a_{\mathbf{2,L,m}}e(\mathbf{r_L}, -t-T_\mathbf{L}+\Delta t_{1,\mathbf{z,L}})$ is $2\Delta t_{1,\mathbf{z,L}}$ When $\boldsymbol{p}>1$, $(4p-2)\Delta t_{1,\mathbf{z,L}} > 2\Delta t_{1,\mathbf{z,L}}$. Therefore, the two signal components contained in (17) get closer to each other, compared to those in (18), as shown in Figure 8. As a result, $I_c(\mathbf{r_z}) \geq I_o(\mathbf{r_z})$, which causes that the -3dB width of the conventional TR localization method is wider than that of the proposed method with $\boldsymbol{p}>1$.

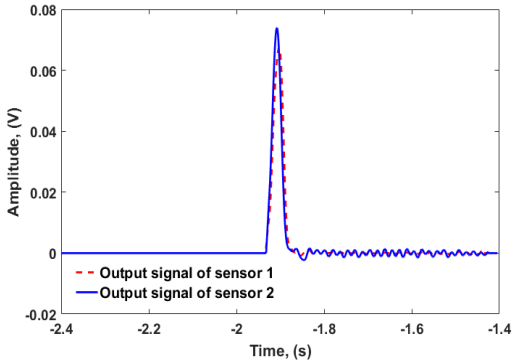

(a)

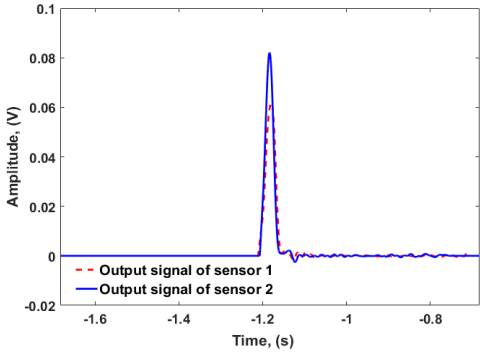

(b)

FIGURE 8. The two sensors' output signals of the conventional time reversal localization method for the two leakages. (a) at 25.6m, leakage L1. (b) at 34m, leakage L2.

V. CONCLUSION

In this paper, a novel localization method is developed to localize the leakage of a pipeline with adjustable resolution. The proposed method designs a time reversal based formula to adjust the localization resolution to optimize the captured leakage signals. The optimized signals and the corresponding back-ground functions are then used to localize the leakages. By using the proposed method, the resolution (−3dB width) can get higher with increase of the parameter $\boldsymbol{p}$ in the time reversal based formula. We applied the proposed localization method to localize leakages in a model gas pipeline. The experimental results demonstrated that the proposed method can localize the leakages in a 55.8m PVC pipeline, with adjustable resolutions. Furthermore, when the parameter $\boldsymbol{p}$=80, the proposed method can provide a −3dB width of 0.03m which is 0.541% of that of the conventional TR localization method. In addition to the pipeline leakage monitoring, the method can also be used for other passive monitoring problems.

REFERENCES

[1] P. Giannelli, A. Bulletti, and L. Capineri, "Multifunctional piezopolymer film transducer for structural health monitoring applications," *IEEE Sensors J.*, vol. 17, no. 14, pp. 4583–4586, Jan. 2017.

[2] M. Fallahpour and R. Zoughi, "Fast 3-D qualitative method for through-wall imaging and structural health monitoring," *IEEE Geosci. Remote Sens. Lett.*, vol. 12, no. 12, pp. 2463–2467, Dec. 2015.

[3] K.-Y. Oh, J.-Y. Park, J.-S. Lee, B. I. Epureanu, and J.-K. Lee, "A novel method and its field tests for monitoring and diagnosing blade health for wind turbines," *IEEE Trans. Instrum. Meas.*, vol. 64, no. 6, pp. 1726–1733, Jun. 2015.

[4] F. G. Baptista and J. V. Filho, "A new impedance measurement system for PZT-based structural health monitoring," *IEEE Trans. Instrum. Meas.*, vol. 58, no. 10, pp. 3602–3608, Oct. 2009.

[5] E. S. De Freitas, F. G. Baptista, D. E. Budoya, and B. A. De Castro, "Equivalent circuit of piezoelectric diaphragms for impedance-based structural health monitoring applications," *IEEE Sensors J.*, vol. 17, no. 17, pp. 5537–5546, Sep. 2017.

[6] H. Hoshyarmanesh, A. Abbasi, P. Moein, M. Ghodsi, and K. Zareinia, "Design and implementation of an accurate, portable, and time-efficient impedance-based transceiver for structural health monitoring," *IEEE/ASME Trans. Metachronics*, vol. 22, no. 6, pp. 2809–2814, Dec. 2017.

[7] V. A. D. De Almeida, F. G. Baptista, and P. R. De Aguiar, "Piezoelectric transducers assessed by the pencil lead break for impedance-based structural health monitoring," *IEEE Sensors J.*, vol. 15, no. 2, pp. 693–702, Feb. 2015.

[8] W. Xu, W. D. Zhu, S. A. Smith, and M. S. Cao, "Structural damage detection using slopes of longitudinal vibration shapes," *J. Vibrat. Acoust.*, vol. 14, no. 5, p. 034501, 2016.

[9] R. B. Bai, W. Ostachowicz, M. S. Cao, and Z. Su, "Crack detection in beams in noisy conditions using scale fractal dimension analysis of mode shapes," *Smart Mater. Struct.*, vol. 23, no. 6, p. 065014, 2014.

[10] M. S. Cao, H. Xu, R. B. Bai, W. Ostachowicz. M. Radzieński, and L. Chen, "Damage characterization in plates using singularity of scale mode shapes," *Appl Phys Lett.*, vol. 106, no. 12, p. 121906, 2015.

[11] H. Huang and T. Bednorz, "Introducing S-parameters for ultrasound-based structural health monitoring," *IEEE Trans. Ultrason., Ferroelect., Freq. Control*, vol. 61, no. 11, pp. 1856–1863, Nov. 2014.

[12] R. M. Levine and J. E. Michaels, "Block-sparse reconstruction and imaging for Lamb wave structural health monitoring," *IEEE Trans. Ultrason., Ferroelect., Freq. Control*, vol. 61, no. 6, pp. 1006–1015, Jun. 2014.

[13] J. Cheng, J. N. Potter, A. J. Croxford, and B. W. Drinkwater, "Monitoring fatigue crack growth using nonlinear ultrasonic phased array imaging," *Smart Mater. Struct.*, vol. 26, no. 5, p. 055006, 2017.

[14] G. Lu, Y. Li, and G. Song, "A delay-and-Boolean-ADD imaging algorithm for damage detection with a small number of piezoceramic transducers," *Smart Mater. Struct.*, vol. 25, no. 9, p. 095030, 2016.

[15] J. Ebrahimi-Zadeh, M. Dehmollaian, and K. Mohammadpour-Aghdam, "Electromagnetic time-reversal imaging of pinholes in pipes," *IEEE Trans. Antennas Propag.*, vol. 64, no. 4, pp. 1356–1363, Apr. 2016.

[16] D. Gao, Z. Wu, L. Yang, and Y. Zheng, "Guide waves-based multi-damage identification using a local probability-based diagnostic imaging method," *Smart Mater. Struct.*, vol. 25, no. 4, p. 045009, 2016.

[17] H. Z. Hosseinabadi, B. Nazari, R. Amirfattahi, H. R. Mirdamadi, and A. R. Sadri, "Wavelet network approach for structural damage identification using guided ultrasonic waves," *IEEE Trans. Instrum. Meas.*, vol. 63, no. 7, pp. 1680–1692, Jul. 2014.

[18] J. Lin, F. Gao, Z. Luo, and L. Zeng, "High-resolution Lamb wave inspection in viscoelastic composite laminates," *IEEE Trans. Ind. Electron.*, vol. 63, no. 11, pp. 6989–6998, Nov. 2016.

[19] Y. An, H. Song, and H. Sohn, "Wireless ultrasonic wavefield imaging via laser for hidden damage detection inside a steel box girder bridge," *Smart Mater. Struct.*, vol. 23, no. 9, p. 095019, 2014.

[20] J. Cai, L. Shi, S. Yuan, and Z. Shao, "High spatial resolution imaging for structural health monitoring based on virtual time reversal," *Smart Mater. Struct.*, vol. 20, no. 5, p. 055018, 2011.

[21] Q. Feng, Q. Kong, L. Huo, and G. Song, "Crack detection and leakage monitoring on reinforced concrete pipe," *Smart Mater. Struct.*, vol. 24, no. 11, p. 115020, 2015.

[22] J. Wan, Y. Yu, Y. Wu, R. Feng, and N. Yu, "Hierarchical leak detection and localization method in natural gas pipeline monitoring sensor networks," *Sensors*, vol. 12, no. 1, pp. 189–214, 2012.

[23] D. Ozevin and Y. Hazim, "New leak localization approach in pipelines using single-point measurement," *J. Pipeline Syst. Eng. Pract.*, vol. 5, no. 2, p. 04013020, 2013.

[24] Z.-G. Jia, L. Ren, H.-N. Li, S.-C. Ho, and G.-B. Song, "Experimental study of pipeline leak detection based on hoop strain measurement," *Structural Control Health Monitor.*, vol. 22, no. 5, pp. 799–812, 2015.

[25] Y. Zhao, X. Zhuang, and S. Min, "A new method of leak location for the natural gas pipeline based on wavelet analysis," *Energy*, vol. 35, no. 9, pp. 3814–3820, 2010.
[26] Q. Hou, L. Ren, W. Jiao, P. Zou, and G. Song, "An improved negative pressure wave method for natural gas pipeline leak location using FBG based strain sensor and wavelet transform," *Math. Problems Eng.*, vol. 2013, p. 278794, 2013.
[27] J. Hu, L. Zhang, and W. Liang, "Detection of small leakage from long transportation pipeline with complex noise," *J. Loss Prevention Process Ind.*, vol. 24, no. 4, pp. 449–457, 2011.
[28] C. Liu, Y.-X. Li, Y.-K. Yan, J.-T. Fu, and Y.-Q. Zhang, "A new leak location method based on leakage acoustic waves for oil and gas pipelines," *J. Loss Prevention Process Ind.*, vol. 35, pp. 236–246, May 2015.
[29] G. Giunta, G. Bernasconi, and S. D. Giudice, "Pipeline monitoring with vibroacoustic sensing," *Mater. Eval.*, vol. 73, no. 7, pp. 979–986, 2015.
[30] J. Zhu, L. Ren, S.-C. Ho, Z. Jia, and G. Song, "Gas pipeline leakage detection based on PZT sensors," *Smart Mater. Struct.*, vol. 26, p. 025022, Jan. 2017.
[31] L. Meng, Y. Li, W. Wang, and J. Fu, "Experimental study on leak detection and location for gas pipeline based on acoustic method," *J. Loss Prevention Process Ind.*, vol. 25, no. 1, pp. 90–102, 2012.
[32] R. K. Ing, N. Quieffin, S. Catheline, and M. Fink, "In solid localization of finger impacts using acoustic time-reversal process," *Appl. Phys. Lett.*, vol. 87, no. 20, p. 204104, 2005.
[33] T.-H. Liao, P.-C. Hsieh, and F.-C. Chen, "Subwavelength target detection using ultrawideband time-reversal techniques with a multilayered dielectric slab," *IEEE Antennas Wireless Propag. Lett.*, vol. 8, pp. 835–838, 2009.
[34] Z.-S. Gong, B.-Z. Wang, Y. Yang, H.-C. Zhou, S. Ding, and X.-H. Wang, "Far-field super-resolution imaging of scatterers with a time-reversal system aided by a grating plate," *IEEE Photon. J.*, vol. 9, no. 1, Feb. 2017, Art. no. 6900108.
[35] M. Rupin, S. Catheline, and P. Roux, "Super-resolution experiments on Lamb waves using a single emitter," *Appl. Phys. Lett.*, vol. 106, no. 2, p. 024103, 2015.
[36] L. Li, F. Li, and T. J. Cui, "Feasibility of resonant metalens for the subwavelength imaging using a single sensor in the far field," *Opt. Exp.*, vol. 22, no. 15, pp. 18688–18697, 2014.
[37] Q. Gao, B.-Z. Wang, and X.-H. Wang, "Far-field super-resolution imaging with compact and multifrequency planar resonant lens based on time reversal," *IEEE Trans. Antennas Propag.*, vol. 63, no. 12, pp. 5586–5592, Dec. 2015.
[38] R. Wang, B.-Z. Wang, Z.-S. Gong, and X. Ding, "Far-field subwavelength imaging with near-field resonant metalens scanning at microwave frequencies," *Sci. Rep.*, vol. 5, Jun. 2015, Art. no. 11131.
[39] D. Ates, A. O. Cakmak, and E. Ozbay, "Near-field light localization using subwavelength apertures incorporated with metamaterials," *Opt. Commun.*, vol. 285, no. 16, pp. 3390–3396, 2012.
[40] A. Grbic and G. V. Elefteriades, "Overcoming the diffraction limit with a planar left-handed transmission-line lens," *Phys. Rev. Lett.*, vol. 92, no. 11, p. 117403, 2004.

GUANGMIN ZHANG received the B.S., M.S., and Ph.D. degrees in electronic engineering from the University of Electronic Science and Technology of China, Chengdu, in 2005, 2008, and 2012, respectively.

He is currently an Assistant Professor with the Department of Electronic Engineering, Dongguan University of Technology. His research interests include the time reversal method, imaging methods, damage detection, and radio technology.

JUNXIAO ZHU received the B.S. and M.S. degrees from the University of Electronic Science and Technology of China in 2005 and 2008, respectively, and the Ph.D. degree from the Department of Mechanical Engineering, University of Houston, Houston, TX, USA, in 2016. He is currently with the Smart Material and Structures Laboratory, University of Houston. His research interests include the mechanism of ultrasonic wave propagation, piezoceramic transducers, machine learning, and structural health monitoring. He is currently serving as the Vice President of the IEEE Ultrasonic, Ferroelectric, and Frequency Control Society, University of Houston Student Branch.

YUE SONG received the B.S. degree from the Beijing University of Posts and Telecommunications, Beijing, in 1988, and the M.S. degree in signal processing from Northwestern Polytechnical University in 1990.

He is currently a Professor with the Department of Electronic Engineering, Dongguan University of Technology. His research interests include embedded system and detection technology.

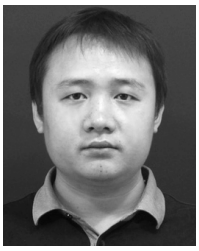

CHAO PENG received the B.S. and M.S. degrees in electronic engineering from Jilin University, Changchun, in 2007 and 2009, respectively, and the Ph.D. degree in electronic engineering from Xiamen University in 2015.

He is currently an Assistant Professor with the Department of Electronic Engineering, Dongguan University of Technology. His research interests include target recognition and sensing technology.

GANGBING SONG received the B.S. degree from Zhejiang University, China, in 1989, and the M.S. and Ph.D. degrees from the Department of Mechanical Engineering, Columbia University, New York City, NY, USA, in 1995 and 1991, respectively. He is the founding Director of the Smart Materials and Structures Laboratory and a Professor of mechanical engineering, civil and environmental engineering, and electrical and computer engineering with the University of Houston. He has developed two new courses in smart materials and published over 400 papers, including 196 peer-reviewed journal articles. He is also an inventor or co-inventor of 12 U.S. patents and 11 pending patents. He is a member of the ASCE and ASME. He was a recipient of the NSF CAREER Award in 2001. He has expertise in smart materials and structures, structural vibration control, piezoceramics, ultrasonic transducers, structural health monitoring, and damage detection. He has received research funding in smart materials and related research from the NSF, DoE, NASA, Department of Education, Texas Higher Education Board, Texas Space Grant Consortium, University of Texas Medical Branch, Ohio Space Grant Consortium, Ohio Aerospace Institute, Ohio Department of Transportation, HP, OptiSolar, GE, and Cameron. In addition to his research effort, he has passion in improving teaching using technology. He received the prestigious Outstanding Technical Contribution Award from the Aerospace Division of ASCE, the Excellence in Research and Scholarship Award at Full Professor Level from UH, the Celebrating Excellence Award for Excellence in Education from International Society of Automation, the IEEE Educational Activities Board Meritorious Achievement Award in Informal Education, among others. He is a Leader in Internet-enabled remote experiment/laboratory and a pioneer in systematically implementing remote experiments in engineering education. He served as the General Chair of the Earth and Space Conference 2010, Aerospace Division, ASCE.